Angga/Footstep_Detection_for_Indoor_Positioning_using_Accelerometer_and_Magnetometer_Sensor_on_Smartphone.pdf

By Angga Pradipta

Footstep Detection for Indoor Positioning using Accelerometer and Magnetometer Sensor on Smartphone

Made Liandana
Study Program Information Technology
Institut Teknologi dan Bisnis STIKOM Bali
Bali, Indonesia
liandana@stikom-bali.ac.id

Bagus Made Sabda Nirmala
Study Program Information Technology
Institut Teknologi dan Bisnis STIKOM Bali
Bali, Indonesia
sabda@stikom-bali.ac.id

Gede Angga Pradipta
Study Program Information System
Institut Teknologi dan Bisnis STIKOM Bali
Bali, Indonesia
angga_prodipta@stikom-bali.ac.id

Dandy Pramana Hostiadi
Study Program Information System
Institut Teknologi dan Bisnis STIKOM Bali
Bali, Indonesia
dandy@stikom-bali.ac.id

Abstract—**Indoor positioning using inertial sensors can be used as an alternative to GPS because indoor GPS signals are weaker than outdoors. Inertial sensors such as accelerometers and magnetometers are already packaged in smartphone devices, so the use of smartphones for indoor positioning is an option. Footstep detection is essential in determining position indoors; in this study, footsteps were detected using the accelerometer sensor. While the heading direction is calculated using the Magnetometer sensor. Previous studies have shown that the position of the smartphone, when held, affects indoor positioning estimated. So in this study, it is proposed to use the angle of inclination. In addition, to identify the initial position, a marker in the form of a QR Code is used. The proposed approach consists of 5 processes, namely: calculating the tilt angle, detection of footsteps, calculating the heading direction, estimated displacement, and the estimation of the position. The error in the position estimation is used as a test parameter. The longer path length results in a smaller error than the shorter path.**

Keywords—Indoor positioning, tilt angle, QR code, accelerometer, magnetometer.

I. INTRODUCTION

Information about the floor plan is necessary, especially for visitors who visit the building for the first time. The floor plan is usually affixed to the room's wall or a corner of the room. However, the floor plan cannot provide up-to-date information on the position of visitors due to the limited number of floor plans posted in the room and the position of visitors who move, so a navigation system is needed. One navigation system technology is the Global Positioning System (GPS) [1]. However, GPS cannot work properly indoor areas due to signal attenuation caused by building materials [2][3][4]. Thus, a navigation system indoors that does not use GPS is required [4][5][6][7][8][9]. Indoor positioning can be grouped based on its technology, namely: optical technology, sound-based technology, radio frequency, hybrid technology, and passive technology [3]. There are examples of optical-based technologies such as Infrared (IR) and Visible Light Communication (VLC) [10][11]. For sound-based technology can use ultrasonic [12]. Indoor positioning technologies that use radio frequencies such as Wi-Fi [13], Bluetooth [14], ZigBee [15] and RFID [16]. While, passive technology generally uses inertial sensors, such as magnetic or magnetometers [17], accelerometers, and gyroscopes [18].

Indoor positioning that uses an inertial sensor is pedestrian navigation [17][18]. Assuming every visitor to a building is a pedestrian, inertial sensors can be used for navigation systems for visitors in a building. Pedestrian navigation techniques that use inertial sensors are also known as Pedestrian Dead Reckoning (PDR). PDR technique combines step detection, stride length estimation, and user direction estimation [19]. The user's position is updated by adding the current relative displacement estimate to the previous position estimate [19].

The smartphone's size, which is relatively small so that it is easy to carry everywhere, is reasonably practical if used for indoor positioning, especially pedestrian navigation systems. In addition, the smartphone has also been installed with several inertial sensors, such as an accelerometer, gyroscope, magnetometer, and other sensors. The inertial sensor contained in the smartphone does not require particular infrastructure if it is used for indoors positioning [20][21][22]. In pedestrian navigation using the PDR technique, the results of position calculations are very dependent on the carrying position of the smartphone device used by the user [23]. Consequently, the user must maintain the smartphone position. For example, the carrying position smartphone is horizontal. Its carrying position flat must be held while calculating the indoor position so that the sensor readings do not change drastically.

Estimation of stride length and estimation of heading are essential parameters for positioning indoors using the PDR technique [4][23][24][25]. Another study combined these parameters with RSS from Wi-Fi and Bluetooth [26][27]. This study combined stride length estimation and heading estimation with smartphone tilt angle. This tilt angle is calculated based on the acceleration generated by the accelerometer sensor. The current indoor position is identified using the acceleration threshold value, compared with the acceleration value generated by the accelerometer sensor when the user steps. The user's

heading uses a compass direction that can be identified using the magnetometer sensor.

II. METHODS

Footstep detection, stride length estimation, and user direction estimation are the main processes in indoor positioning using the PDR technique [19]. In addition, the carrying position of a smartphone is also essential [23]. Therefore, the PDR technique is combined with reading the tilt angle. In this study, the sampling rate of the accelerometer sensor is 60 Hz. The indoor positioning process is shown in Fig 1.
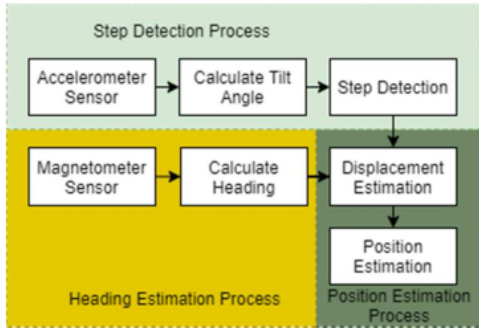

Fig. 1. Indoor Positioning Process

A. Tilt Angle

The acceleration generated by the accelerometer sensor is used to calculate the tilt angle of the smartphone held by the user. The tilt angle can be calculated using Eq. (1), also used in the previous study [28].

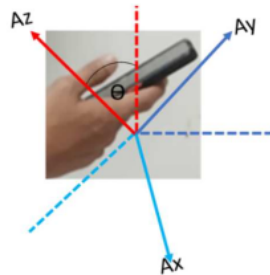$$\theta = tan^{-1}\left(\frac{\sqrt{Ax^2 + Ay^2}}{Az}\right)\frac{180}{\pi} \qquad (1)$$

Fig. 2. Til Angle of Smartphone Position

As shown in Fig 2, the dotted line is the direction of the accelerometer sensor's axis (x,y,z); when the smartphone is placed horizontally, the line is used as a reference point. While the arrows indicate the direction of the axis when held by the user. When the user uses a smartphone in a position shown in Fig 2, the resulting angle ranges from 15 to 40 degrees. The angle value is used as the minimum angle threshold value θth_{min} and the maximum angle threshold value θth_{max}.

B. Step Detection

The acceleration generated by the three axes of the accelerometer sensor is used to calculate the Signal Vector Magnitude (SVM). In the previous study [29][30][31], the SVM signal was calculated using equation (2). Ax, Ay, and Az are accelerometer acceleration values for the x, y, and z axes, while SVM is the square root of the sum of the squares of each axle.

$$SVM = \sqrt{(A_x)^2 + (A_y)^2 + (A_z)^2} \qquad (2)$$

Gravity contributes to the acceleration value on each axis of the accelerometer sensor; in this study, the contribution of the value of gravity is reduced by using a filter. Filtering is done by software using the program code provided on the official Android Developer website [32]. Thus, in this study, the SVM value is calculated using equation (3). $SVM_{fil}(i)$ is the square root of the sum of the squares of each filtered axis at the i-th sampling point. Meanwhile, $Ax_{fil}(i)$, $Ay_{fil}(i)$, and $Az_{fil}(i)$ are the x, y, and z axis acceleration values that have been filtered at the i sampling point.

$$SVM_{fil}(i) = \sqrt{(Ax_{fil}(i))^2 + (Ay_{fil}(i))^2 + (Az_{fil}(i))^2} \qquad (3)$$

where $i = 1$ to 30

Each one-step movement will produce an SMV filter pattern, as shown in Fig.3 (which is flanked by a yellow line); the resulting pattern is in the range of 30 sampling points so that the i sampling point in Eq. (2) starts from 1 to 30. The range of sampling points is referred to as the sampling length, denoted by n. The assumption is that all footsteps are steps forward.
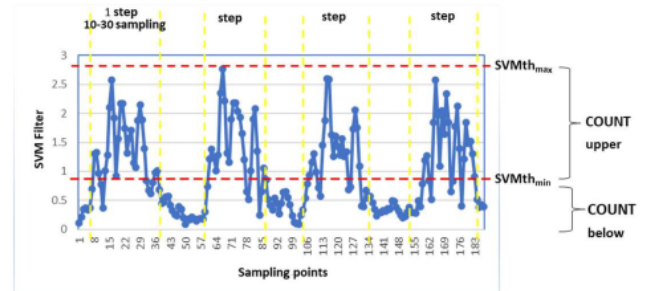

Fig. 3 Sampling of Walking.

In addition to using the SVM filter value, the parameter used to detect footsteps is the difference from the SVM filter, which is calculated using Eq. (4). SVM$diff$(i) is the difference of the SVM filter at the i sampling point starting from 1 to n-1.

$$SVM_{diff}(i) = SVM_{fil}(i + 1) - SVM_{fil}(i) \qquad (4)$$

The value of the SVM filter during one step ranges from 0.8 to 2.75, as shown in Figure 3 (red line), and SVM$diff$ is smaller or equal to 2. The value of 0.8 is used as minimum threshold for SVM$thmin$, and the value of 2.75 is the maximum threshold for SVM$thmax$. The flow for detecting a single footstep is as follows:

(1) Read the x, y, and z axis acceleration data from the smartphone's accelerometer sensor.

(2) Calculate the angle of inclination using equation (1).

(3) If $\theta th_{min} \leq \theta \leq \theta th_{max}$, calculate the SVM filter (SVM_{fil}) using Eq. (3). Steps (1) to (3) are repeated so that the number of sampling is equal to n (30 samplings).

(4) Calculate the difference in SVM filter (SVM_{diff}) using Eq. (4).

(5) Trace SVM_{diff} from 1 to n-1 sampling. If there is a difference greater than 2 (threshold), it is possible that the sampling value that has been taken is not a pattern of one footstep, repeat sampling from step (1). However, if the SVM_{diff} difference is less than or equal to 2, go to step 6.

(6) Trace SVM_{fill} from 1st to n sampling. One step is detected if there are 5 to 10 values that meet $SVMth_{min} \leq SVM_{fill} \leq SVMth_{max}$ ($COUNT_{upper}$) and there are 3 to 10 values that meet $SVM_{fil} < SVMth_{min}$ ($COUNT_{below}$).

```
Pseudo code step detection method
N (Number of sampling)= 30
θthₘᵢₙ= 15
θthₘₐ= 40
diffₜₕ=2
WHILE(Read Sensor):
   INPUT: Ax₍ᵢ₎, Ay₍ᵢ₎, Az₍ᵢ₎(until i=N)
   Calculate Axfil₍ᵢ₎, Ayfill₍ᵢ₎, Azfill₍ᵢ₎
   FOR i = 1 to N
        Calculate tilt angle θ
        IF θthₘᵢₙ ≤ θ ≤ θthₘₐₓ THEN
              Calculate SVMfill₍ᵢ₎
        ENDIF
   ENDFOR
   FOR i = 1 to N
      Calculate SVMdiff
      IF SVMdiff₍ᵢ₎ < diffₜₕ THEN
         IF SVMthₘᵢₙ ≤ SVMfill₍ᵢ₎ ≤ SVMthₘₐₓ
                       THEN
               COUNTupper= COUNTupper+1
         ELSEIF SVMfill₍ᵢ₎ < SVMthₘᵢₙ THEN
               COUNTbelow=COUNTbelow +1
         ENDIF
       ENDIF
      ENDFOR
      IF (5 > COUNTupper >10)
              AND (3 > COUNTbelow > 10) THEN
         STEP = TRUE
         REMOVE all index of Axᵢ, Ayᵢ, Azᵢ
      ELSE
         STEP= FALSE
         REMOVE first index of Axᵢ, Ayᵢ, Azᵢ
      ENDIF
ENDWHILE
```

C. Calculate Heading

The heading direction of smartphone users is detected using the Magnetometer sensor on the smartphone. The values of the Magnetometer sensor are converted into an azimuth angle. The azimuth value obtained is divided into four parts, as shown in Fig 4, each part is used to estimate the user's heading direction.
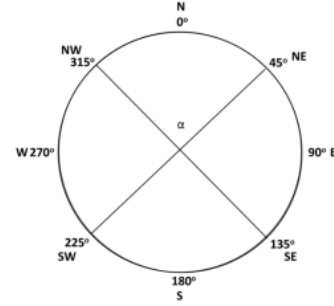
Fig. 4. Azimuth

D. Displacement Estimation

The estimated displacement from one point to the next is known based on detected footsteps. So, the length of the footstep determines how much the value of the displacement that occurs. Therefore, it is necessary to find a way to determine the length of the stride. Estimation of stride length can use static and dynamic approaches [30][33][34]. One of the popular models for estimating stride length is the Weinberg model [35], which is defined using Eq. (5).

$$Step\_Length = k \times \sqrt[4]{a_{max} + a_{min}} \qquad (5)$$

k is a constant, while a_{max} dan a_{min} are the minima and maximum values of acceleration. Ho et al. [34], dynamically calculate k using Eq. (6), where $\bar{\upsilon}_{step}$ is the average velocity magnitude on the accelerometer sensor's x, y, and z axes at each step. To calculate $\bar{\upsilon}_{step}$ using equations (7), (8), (9), and (10).

$$k = 0.68 - 0.37 \times \bar{\upsilon}_{step} + 0.15 \times \bar{\upsilon}^2_{step} \qquad (6)$$

$$\bar{\upsilon}_{step} = \sqrt{(\bar{\upsilon}_{stepX})^2 + (\bar{\upsilon}_{stepY})^2 + (\bar{\upsilon}_{stepZ})^2} \qquad (7)$$

Chronologically, $\bar{\upsilon}_{stepX}$, $\bar{\upsilon}_{stepY}$, dan $\bar{\upsilon}_{stepZ}$ are the average velocity on the x, y, and z axes with a sampling point length of 30. The current velocity value is updated using the previous velocity value, while the time interval is obtained from 1 divided by the sampling rate sensor, which is 60 Hz.

$$\bar{\upsilon}_{stepX} = \frac{1}{30} \sum_{i=1}^{30} \left(\bar{\upsilon}_{stepX}(i-1) + (Ax_{fil}(i) \times \frac{1}{60})\right) \qquad (8)$$

$$\bar{\upsilon}_{stepY} = \frac{1}{30} \sum_{i=1}^{30} \left(\bar{\upsilon}_{stepY}(i-1) + (Ay_{fil}(i) \times \frac{1}{60})\right) \qquad (9)$$

$$\bar{\upsilon}_{stepZ} = \frac{1}{30} \sum_{i=1}^{30} \left(\bar{\upsilon}_{stepZ}(i-1) + (Az_{fil}(i) \times \frac{1}{60})\right) \qquad (10)$$

Furthermore, using the Weinberg model, the k_{step} value is used to calculate the step length (L) so that equation (5) is rewritten into equation (11). Where max($SVMfil$) and min($SVMfil$) respectively, are the maximum and minimum values of SVM_{fil} that are found throughout 30 sampling points.

$$L = k_{step} \times \sqrt[4]{max(SVM_{fil}) + min(SVM_{fil})} \qquad (11)$$

E. Position Estimation

The user's position in the room is presented on a smartphone screen display as a two-dimensional floor plan. Thus, a comparison scale is needed between the actual room size and a two-dimensional room plan. The displacement in one footstep will be represented by the displacement of the point in several pixels on the smartphone screen; the displacement of the point follows the coordinate system on the smartphone screen. The displacement is calculated using equations 12 and 13.

$$S_x = L \times \frac{l_m}{l_r} \qquad (12)$$

$$S_y = L \times \frac{p_m}{p_r} \qquad (13)$$

S_x and S_y are the value of point displacement in pixels on the x and y axes of the smartphone screen. While l_m and p_m are the length and width of a two-dimensional plan that represents the shape of the room in pixel size. For l_r and p_r are the length and width of the room. S_x and S_y are calculated if footsteps are detected. As shown in TABLE I, S_x and S_y are used to update the current positions of x and y, while x_0 and y_0 are the previous positions.

TABLE I. UPDATE POSITION IN FLOOR MAPS SMARTPHONE

No	Azimuth (α)	Current position
1	$0 \leq \alpha \leq 45$ and $315 \leq \alpha \leq 359$	x=x$_0$, y=y$_0$ + Sy
2	$45 < \alpha < 135$	x= x$_0$ - S$_x$, y= y$_0$
3	$135 \leq \alpha < 225$	x= x$_0$, y= y$_0$ - Sy
4	$225 \leq \alpha \leq 315$	x= x$_0$ + S$_x$, y=y$_0$

III. RESULT AND DISCUSSION

The smartphone Model M1804C3DG is used as the test device. Its device has an Octa-Core Max 2.00 GHz processor, a screen size of 720 x 1440 pixels, and an accelerometer sampling rate of 60 Hz. Participants use the same device to perform the test scenarios.

A. Map of Building

The building presented in map form does not point to the north exactly but has an angle difference of 8°, as shown in Fig. 5. So before the movement value is updated, the angle in Table 1 is reduced by 8° using equation (14).

$$\alpha = \alpha - 8^o \qquad (14)$$

Fig. 5. Floor plans

Pedestrian navigation using the PDR technique requires a reference point as the initial position. In this study, to determine the starting position, smartphone users must scan a QRcode. The QRcode contains information on the position of the x and y-axis maps which are presented in the smartphone application. The QRcode label is placed in an easy-to-reach position and is the first point found by users visiting the building, for example, the exit/entrance of elevators and stairs.

B. Footstep Detection Test

The technique used to detect footsteps was performed on two participants, one male and one female, with a profile as shown in Table 2. Each participant took 7 test scenarios with a total of 280 steps. Each scenario takes a different number of steps, as shown in Table 3.

TABLE II. PARTICIPANT PROFILE

Participant	Gender	Height (cm)	Weight (kg)
1	Male	170	70
2	Famale	150	50

TABLE III. PARTICIPANT TEST

No.	Atcual Step	Detected steps	
		Participant 1	Participant 2
1	5	6	6
2	10	9	11
3	15	17	17
4	25	26	28
5	50	53	60
6	75	80	83
7	100	97	110

$$\% \ error = \frac{|actual \ step - detected \ step|}{actual \ step} \ x \ 100\% \qquad (15)$$
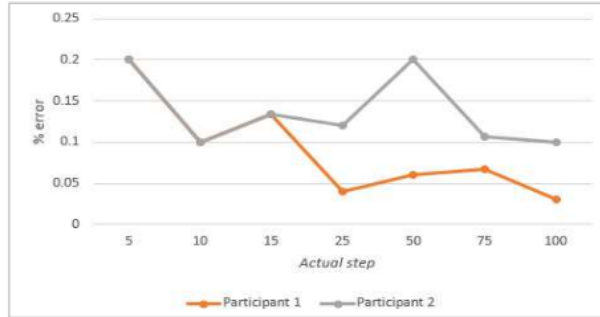
Fig. 6. Error percentage

The error percentage of each test scenario is calculated using equation (15). Fig 6 shows the percentage of errors decreases when the number of steps increases. This is probably due to the pattern of steps at the beginning of the walking; the acceleration value is irregular.

C. Floor plans of the test.

The initial position is known based on the QRcode installed at a certain point in the room (Fig. 7(a)). The smartphone is held while maintaining a tilt angle of 15 to 40 degrees, as shown in Fig. 7(b). For the user to know the tilt angle, the application presents the tilt angle of the smartphone held by the user, as shown in Fig. 8

(a) Scan initial position   (b) Smartphone was placed in the hand

Fig. 7. Experimental Scenario

Fig. 8 App shows position and tilt angle

The test line is made by drawing a straight line from the Qrcode point to the next QRcode; then, the line is used as a reference point for the test plan path. Fig. 9 shows the results of the test position and the test plan. The green dotted line indicates the actual position path, while the red dotted line represents the planned path. When testing, the subject moves from the origin (o) to destination (d) through a planned path.

(a) Path testing 1   (b) Path testing 2

(c) Path testing 3   (d) Path testing 4

(0,0)   x   ----- planned path   o   origin

axis direction   ----- test result path   d   destination

y

Fig. 9. Path testing and results

Four test paths have been carried out; the first test path has a length of 74.5 m, the second test path has a length of 59.7 m, and the third test path has a length of 32.5 m, while the fourth test track has a length of 48.5 m. The test results are calculated using equation (16), $x_{planned}$ and $y_{planned}$ are the positions on the planned x and y coordinates. While $x_{estimated}$ and $y_{estimated}$ are the positions of the estimated results on the x, and y coordinates, respectively. These x and y are the coordinate systems on the smartphone screen.

$$error(i) = \sqrt{\frac{|x_{planned(i)} - x_{estimated(i)}| +}{|y_{planned(i)} - y_{estimated(i)}|}} \qquad (16)$$

The error on each test path is shown in TABLE IV. Fig 10 shows that when the path length is shorter, there is a tendency for error to be greater than when the path is longer. It may be affected by the irregularity of the acceleration value when starting the footstep.

TABLE IV. PATH TESTING RESULTS

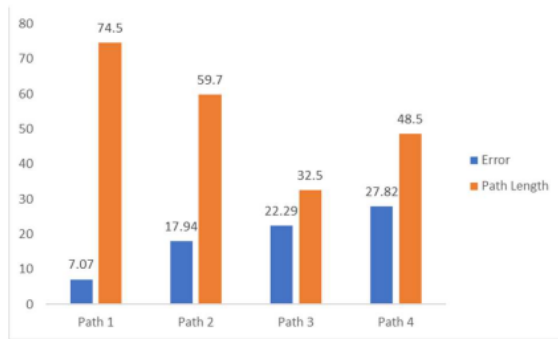| Path	Error
1	7.07
2	17.94
3	22.29
4	27.82

Fig. 10. Error and path length

IV. CONCLUSIONS

The initial position is identified from the information contained in the QRCode. When the smartphone is used to estimate the indoor positioning, the tilt angle is maintained at 15 to 40 degrees. The length of the sampling point from the acceleration of the accelerometer sensor is evaluated to calculate a step of 30 sampling points or half of the sensor's sampling rate. To determine whether the occurrence of a step or not is based on a threshold value. The test is carried out by calculating the error of the position estimation. The test results show that the longer path length produces a smaller error than the shorter path.

This study uses the maximum and minimum threshold values statically to detect the occurrence of steps and only detect forward steps. Using threshold values dynamically and detecting backward steps can be potential for future work.

REFERENCES

[1] S. Haykin, "Cognitive radio: brain-empowered wireless communications," *IEEE J. Sel. Areas Commun.*, vol. 23, no. 2, pp. 201–220, Feb. 2005.

[2] Xin-Yu Lin, Te-Wei Ho, Cheng-Chung Fang, Zui-Shen Yen, Bey-Jing Yang, and Feipei Lai, "A mobile indoor positioning system based on iBeacon technology," in *2015 37th Annual International Conference of the IEEE Engineering in Medicine and Biology Society (EMBC)*, 2015, pp. 4970–4973.

[3] R. F. Brena, J. P. García-Vázquez, C. E. Galván-Tejada, D. Muñoz-Rodriguez, C. Vargas-Rosales, and J. Fangmeyer, "Evolution of Indoor Positioning Technologies: A Survey," *J. Sensors*, vol. 2017, pp. 1–21, Mar. 2017.

[4] X. Gan, B. Yu, Z. Heng, L. Huang, and Y. Li, "Indoor combination positioning technology of Pseudolites and PDR," in *2018 Ubiquitous Positioning, Indoor Navigation and Location-Based Services (UPINLBS)*, 2018, pp. 1–7.

[5] L. Yu, Y. Liu, T. Chi, and L. Peng, "An iBeacon-based indoor and outdoor positioning system for the fire emergency command," in *2017 Forum on Cooperative Positioning and Service (CPGPS）*, 2017, pp. 326–329.

[6] Z. Li and J. Huang, "Study on the use of Q-R codes as landmarks for indoor positioning: Preliminary results," in *2018 IEEE/ION Position,*

Location and Navigation Symposium (PLANS), 2018, pp. 1270–1276.

[7] J. Paek, J. Ko, and H. Shin, "A Measurement Study of BLE iBeacon and Geometric Adjustment Scheme for Indoor Location-Based Mobile Applications," *Mob. Inf. Syst.*, vol. 2016, pp. 1–13, Oct. 2016.

[8] W. Shao *et al.*, "Location Fingerprint Extraction for Magnetic Field Magnitude Based Indoor Positioning," *J. Sensors*, vol. 2016, pp. 1–16, Dec. 2016.

[9] G. Feng, L. Ma, and X. Tan, "Visual Map Construction Using RGB-D Sensors for Image-Based Localization in Indoor Environments," *J. Sensors*, vol. 2017, pp. 1–18, Oct. 2017.

[10] E. M. Gorostiza, J. L. Lázaro Galilea, F. J. Meca Meca, D. Salido Monzú, F. Espinosa Zapata, and L. Pallarés Puerto, "Infrared Sensor System for Mobile-Robot Positioning in Intelligent Spaces," *Sensors*, vol. 11, no. 5, pp. 5416–5438, May 2011.

[11] K. Y. Yi, D. Y. Kim, and K. M. Yi, "Development of a Localization System Based on VLC Technique for an Indoor Environment," *J. Electr. Eng. Technol.*, vol. 10, no. 1, pp. 436–442, Jan. 2015.

[12] A. De Angelis *et al.*, "Design and characterization of an ultrasonic indoor positioning technique," in *2014 IEEE International Instrumentation and Measurement Technology Conference (I2MTC) Proceedings*, 2014, pp. 1623–1628.

[13] Z.-A. Deng, Z. Qu, C. Hou, W. Si, and C. Zhang, "WiFi Positioning Based on User Orientation Estimation and Smartphone Carrying Position Recognition," *Wirel. Commun. Mob. Comput.*, vol. 2018, pp. 1–11, Sep. 2018.

[14] P. Kriz, F. Maly, and T. Kozel, "Improving Indoor Localization Using Bluetooth Low Energy Beacons," *Mob. Inf. Syst.*, vol. 2016, pp. 1–11, Apr. 2016.

[15] Z. Dong, C. Mengjiao, and L. Wenjuan, "Implementation of indoor fingerprint positioning based on ZigBee," in *2017 29th Chinese Control And Decision Conference (CCDC)*, 2017, pp. 2654–2659.

[16] H. Kong and B. Yu, "A Moving Object Indoor Tracking Model Based on Semiactive RFID," *Math. Probl. Eng.*, vol. 2018, pp. 1–7, Dec. 2018.

[17] D. Pham and Y. Suh, "Pedestrian Navigation Using Foot-Mounted Inertial Sensor and LIDAR," *Sensors*, vol. 16, no. 1, p. 120, Jan. 2016.

[18] S. Kaiser and C. Lang, "Detecting elevators and escalators in 3D pedestrian indoor navigation," in *2016 International Conference on Indoor Positioning and Indoor Navigation, IPIN 2016*, 2016.

[19] Z. Deng, X. Liu, Z. Qu, C. Hou, and W. Si, "Robust Heading Estimation for Indoor Pedestrian Navigation Using Unconstrained Smartphones," 2018.

[20] P. Zhang, Q. Zhao, Y. Li, X. Niu, Y. Zhuang, and J. Liu, "Collaborative WiFi Fingerprinting Using Sensor-Based Navigation on Smartphones," *Sensors*, vol. 15, no. 7, pp. 17534–17557, Jul. 2015.

[21] Z. Xiao, H. Wen, A. Markham, and N. Trigoni, "Robust indoor positioning with lifelong learning," *IEEE J. Sel. Areas Commun.*, vol. 33, no. 11, pp. 2287–2301, Nov. 2015.

[22] M. Zhou, Y. Tang, W. Nie, L. Xie, and X. Yang, "GrassMA: Graph-Based Semi-Supervised Manifold alignment for Indoor WLAN Localization," *IEEE Sens. J.*, vol. 17, no. 21, pp. 7086–7095, Nov. 2017.

[23] Y. Guo, Q. Liu, X. Ji, S. Wang, M. Feng, and Y. Sun, "Multimode Pedestrian Dead Reckoning Gait Detection Algorithm Based on Identification of Pedestrian Phone Carrying Position," 2019.

[24] J. Geng, L. Xia, J. Xia, Q. Li, H. Zhu, and Y. Cai, "Smartphone-Based Pedestrian Dead Reckoning for 3D Indoor Positioning," *Sensors (Basel).*, vol. 21, no. 24, Dec. 2021.

[25] Y. Liu, Q. Gong, S. Wang, L. Zhang, and F. Xu, "An Outdoor Pedestrian Localization Scheme Fusing PDR and VPR," *Wirel. Commun. Mob. Comput.*, vol. 2022, pp. 1–12, Aug. 2022.

[26] M. Martínez del Horno, L. Orozco-Barbosa, and I. García-Varea, "A smartphone-based multimodal indoor tracking system," *Inf. Fusion*, vol. 76, pp. 36–45, Dec. 2021.

[27] K. Yan, R. Chen, G. Guo, and L. Chen, "Locating Smartphone Indoors by Using Tightly Coupling Bluetooth Ranging and Accelerometer Measurements," *Remote Sens. 2022, Vol. 14, Page 3468*, vol. 14, no. 14, p. 3468, Jul. 2022.

[28] J. Zhu, W. Wang, S. Huang, and W. Ding, "An Improved Calibration

Technique for MEMS Accelerometer-Based Inclinometers," *Sensors 2020, Vol. 20, Page 452*, vol. 20, no. 2, p. 452, Jan. 2020.

[29]   Q. T. Huynh, U. D. Nguyen, L. B. Irazabal, N. Ghassemian, and B. Q. Tran, "Optimization of an Accelerometer and Gyroscope-Based Fall Detection Algorithm," 2015.

[30]   W. Lu, F. Wu, H. Zhu, and Y. Zhang, "A step length estimation model of coefficient self-determined based on peak-valley detection," *J. Sensors*, vol. 2020, 2020.

[31]   Y.-C. Lai, C.-C. Chang, C.-M. Tsai, S.-C. Huang, and K.-W. Chiang, "A Knowledge-Based Step Length Estimation Method Based on Fuzzy Logic and Multi-Sensor Fusion Algorithms for a Pedestrian Dead Reckoning System," *ISPRS Int. J. Geo-Information 2016, Vol. 5, Page 70*, vol. 5, no. 5, p. 70, May 2016.

[32]   A. Developer, "Motion sensors | Android Developers." [Online]. Available: https://developer.android.com/guide/topics/sensors/sensors_motion. [Accessed: 02-Jul-2021].

[33]   A. Abadleh, E. Al-Hawari, E. Alkafaween, and H. Al-Sawalqah, "Step detection algorithm for accurate distance estimation using dynamic step length," in *Proceedings - 18th IEEE International Conference on Mobile Data Management, MDM 2017*, 2017, pp. 324–328.

[34]   N. H. Ho, P. H. Truong, and G. M. Jeong, "Step-Detection and Adaptive Step-Length Estimation for Pedestrian Dead-Reckoning at Various Walking Speeds Using a Smartphone," *Sensors (Basel).*, vol. 16, no. 9, Sep. 2016.

[35]   H. Weinberg, *Using the ADXL202 in Pedometer and Personal Navigation Applications*. Norwood, MA, USA,: Analog Devices, Inc., 2002.

Angga/Footstep_Detection_for_Indoor_Positioning_using_...

ORIGINALITY REPORT

2%
SIMILARITY INDEX

PRIMARY SOURCES

1   eprints.utm.my
    Internet
           75 words — 2%

EXCLUDE QUOTES	ON	EXCLUDE SOURCES	< 2%
EXCLUDE BIBLIOGRAPHY	ON	EXCLUDE MATCHES	OFF